

A novel recurrent mutation in CFAP47 causes male infertility with asthenoteratozoospermia

Mohan Liu¹, Siyu Dai¹, Jiying Zhang², Yanting Yang¹, Chuan Jiang¹, Yihong Yang¹, Hongqian Liu¹, and Ying Shen¹

¹Sichuan University West China Second University Hospital

²Sichuan University West China Hospital

June 6, 2022

Abstract

Multiple morphological abnormalities of the sperm flagella (MMAF) is an important cause of male infertility and is defined as absent, short, coiled, bent irregular flagella. In this study, we identified a novel missense mutation (c.1414G>A; p.V472M) in *Cilia and flagella associated protein 47* (*CFAP47*, NG_016381.2) in two unrelated patients with asthenoteratozoospermia. In addition to the typical MMAF phenotype very analogous to that of *Cfap47* mutant male mice, the two patients also presented abnormal morphology of sperm heads, mitochondrial sheath disorganization, and defects of sperm annulus. Further functional experiments confirmed that the expression of *CFAP47* was markedly reduced in the spermatozoa of the patients. Moreover, coimmunoprecipitation and immunofluorescence showed that *CFAP47* might regulate *CFAP65* and *CFAP69* through physical interactions and is thus involved in sperm morphogenesis. In conclusion, we reveal a novel recurrent mutation in *CFAP47* and further expand the clinical and mutational spectrum of *CFAP47*, finally providing important guidance for genetic counseling and targeted treatment.

1 INTRODUCTION

The etiology of male infertility is highly heterogeneous, and genetic factors account for at least 15% of cases (Jiao et al., 2021). The integrity of the flagella is crucial for sperm motility, and any structural and functional defects of sperm flagella could impair sperm function, which is indispensable for spontaneous fertilization (Inaba et al., 2011). Multiple morphological abnormalities of the sperm flagella (MMAF) is a rare asthenoteratozoospermia with severely impaired sperm motility (Ben et al., 2014). This conception was initially reported in 2014 and has attracted increasing attention (Ben et al., 2014). Recent research based on animal models and genetic analysis has uncovered certain disease-causing or disease-promoting genes. To date, 23 MMAF-associated genes have been identified, including *AK7* (MIM: 615364), *ARMC2* (MIM:618424), *CEP135* (MIM: 611423), *CFAP43* (MIM: 617558), *CFAP44* (MIM: 617559), *CFAP47* (MIM: 301057), *CFAP58* (MIM: 619129), *CFAP65* (MIM: 614270), *CFAP69* (MIM: 617949), *CFAP70* (MIM: 618661), *CFAP91* (MIM: 609910), *CFAP251* (MIM: 618146), *DNAH1* (MIM: 603332), *DNAH2* (MIM: 603333), *DNAH6* (MIM: 603336), *DNAH8* (MIM: 603337), *DNAH17* (MIM: 610063), *DZIP1* (MIM: 608671), *FSIP2* (MIM: 618153), *QRICH2* (MIM: 618304), *SPEF2* (MIM: 610172), *TTC21A* (MIM: 611430), and *TTC29* (MIM: 618735) (Jiao et al., 2021; Toure´ et al., 2020). However, mutations in each gene are possibly responsible for only a small fraction of pathogenic factors, and a mass of cases could not be explained. Therefore, a more comprehensive investigation of the pathology and molecular mechanisms of MMAF is needed to further boost diagnosis efficacy.

The cilia and flagella-associated protein (CFAP) protein family is associated with the development and function of sperm flagellum (Tang et al., 2017). This family plays an important role in the generation,

assembly, and maintenance of motor functions of cilia and flagella. To date, multiple CFAP gene deficiencies have been reported to be associated with MMAF, such as several mutations in *CFAP43*, *CFAP44*, *CFAP58*, *CFAP65*, *CFAP69*, *CFAP70*, and *CFAP251* (Tang et al., 2017; Coutton et al., 2018; Li et al., 2020; He et al., 2020; He et al., 2019; Beurois et al., 2019; Auguste et al., 2018). To date, only one report revealed that cilia and flagella-associated protein 47 (*CFAP47*, NG_016381.2) leads to MMAF in an X-chromosome-linked inheritance pattern (Liu et al., 2021). Males with hemizygous *CFAP47* variants exhibit a typical MMAF phenotype, and the ultrastructure shows an abnormal axoneme, including disorganized outer dense fibers (ODF), and peripheral microtubule doublets (DMTs), as well as central pair of microtubules (CPs), are missing (Liu et al., 2021). *CFAP47* -mutated male mice are sterile, with decreased sperm motility and abnormal flagella morphology (Liu et al., 2021). Hence, future studies should evaluate *CFAP47* in larger cohorts to corroborate the relationship between genotype and phenotype.

Herein, we report two MMAF patients who carried a novel hemizygous mutation c.1414G>A [p.V472M] in *CFAP47*. Bioinformatics analysis and functional studies in vitro validated the pathogenicity of the mutation. Furthermore, we first revealed that *CFAP47* mutations are also related to malformed sperm heads and annulus, as well as suggested the potential mechanism by which *CFAP47* regulates spermatogenesis. Our work provides strong evidence to confirm the causative relationship between *CFAP47* variants and MMAF.

2 MATERIALS AND METHODS

2.1 Study participants and sample collection

The two infertile patients and their parents were enrolled at the West China Second University Hospital of Sichuan University, and these patients all had normal chromosomal karyotypes (46, XY). No large-scale deletions were found in the Y chromosome. This study was conducted following the tenets of the Declaration of Helsinki, and ethical approval was obtained from the Ethical Review Board of West China Second University Hospital, Sichuan University. Written informed consent was obtained from each study participant prior to sample collection.

2.2 Genetic analysis

Peripheral whole blood samples were collected from patients and their parents for genetic analyses. Genomic DNA was isolated from peripheral blood samples of subjects using a whole blood DNA-purification kit (51104, QIAGEN). WES and bioinformatics analyses were performed on the patients' samples. One microgram of genomic DNA was utilized for exon capture using the Agilent Sure Select Human All Exon V6 Kit (Agilent Technologies) and sequenced on the Illumina HiSeq X system (Illumina). Targeted testing of the potentially pathogenic variants in the patients' parents was performed by Sanger sequencing. PCR amplification was accomplished with Dyad Polymerase (Bio-Rad Laboratories), and the PCR products were sequenced on an ABI377A DNA sequencer (Applied Biosystems). The primers used in PCR analysis were as follows: F, 5'-ACCATTATGAGCTAGCTTTCCTT-3'; and R, 5'-ACAGTAACAACAAAGCCAGGT-3'.

2.3 Western blotting

Proteins were extracted from sperm cells. Protein quantitation was performed by BCA Protein Assay (23227, Thermo Fisher) according to the manufacturer's instructions. Next, the proteins were denatured at 95°C for 10 min. The denatured proteins were separated on 10% SDS-polyacrylamide gels (stock gel: 60 V, 30 min; separating gel: 120 V, 1.0 h) and then transferred into a 0.45 µm pore size polyvinylidene difluoride (PVDF) membrane (ISEQ, 00010, Millipore) by wet transfer. The transferred membrane was blocked with 5% skimmed milk for 1 h at room temperature and incubated in primary antibody: anti-CFAP47 (1:500, sc-514714, Santa Cruz Biotechnology); anti-GAPDH (1:1000, ab8245, Abcam) solution at 4°C overnight. Subsequently, the membrane was washed with 1 × TBST three times, and each time, the membrane was cleaned for 5 min. Then, the membrane was incubated with goat anti-mouse IgG secondary antibody-HRP (1:5000, 32230, Thermo Fisher Scientific) in 5% skimmed milk at room temperature for 1.5 h, and the next step was to wash the membrane with 1 × TBST three times. The time for cleaning the membrane was the same as above. Finally, immunoblots were developed using Thermo Scientific Pierce ECL Western Blotting

Substrate (TWBKLS0500, Millipore).

2.4 Immunofluorescence (IF) staining

The sperm from patients and the normal controls and mouse sperm cells were fixed in 4% paraformaldehyde, permeabilized with 0.3% Triton X-100 for 10 min, and blocked with 5% BSA or 30% donkey serum for 60 min at room temperature. The slides were then sequentially incubated with primary antibodies at 4degC overnight. The primary antibodies used were anti-CFAP47 (1:50) and α -tubulin (1:100, A11126, Thermo Fisher Scientific). The next day, 1 \times PBS was used to wash the samples three times. Then, the samples were incubated with AlexaFluor 594 anti-rabbit secondary antibodies (1:1000, 1927937, Thermo Fisher) and AlexaFluor 488 anti-mouse secondary antibodies (1:1000; A32723, Thermo Fisher) for 2 h at room temperature or coincubated with peanut agglutinin (PNA, 1:50, RL-1072-5, Vector), CFAP65 (1:50, HPA055156, Sigma-Aldrich), CFAP69 (1:50, bs-15278R-A647, Bioss), COXIV (1:50, 11242-1-AP, Proteintech) and SEPTIN4 (1:50, 12476-1-AP, Proteintech). Subsequently, 1 x PBS was used to wash the slides three times. Then, the slides were counterstained with 4,6-diamidino-2-phenylindole (DAPI, D9542-1MG, Sigma-Aldrich) to label the nuclei. Finally, the slides were sealed in coverslips. Images were obtained by a laser scanning confocal microscope (Olympus). For immunofluorescence staining of mouse and human testes, after careful xylene dewaxing and gradient ethanol rehydration, the tissue sections were submerged in boiling 10 mM citrate buffer (pH 6.0) for 10 min. Then, the sections were cooled to room temperature and washed with 1 x PBS for 5 min. Subsequently, the sections were treated with 3% hydrogen peroxide solution for 10 min. After washing with 1x PBS, the slides were blocked with 10% normal donkey serum for 30 min and incubated with primary antibodies at 4degC overnight and with Alexa Fluor 488 or Alexa Fluor 594 antibodies for an additional 2 h at room temperature. The primary antibodies used were anti-CFAP47 (1:50), anti-CFAP65 (1:50) and anti-CFAP69 (1:50). Slides of testicular tissues were observed using an LSM800 confocal microscope (Carl Zeiss AG).

2.5 Electron microscopy and concentrated Papanicolaou staining

For scanning electron microscopy (SEM), the sperm samples were centrifuged at 400xg for 10 min at room temperature. The supernatants were carefully aspirated, and the pellets were suspended and fixed in 2.5% glutaraldehyde for 30 min at 4degC. Next, the samples were evenly spread onto 20-mm-diameter slides and fixed in 2.5% glutaraldehyde overnight at 4degC. Following primary fixation, the slides were washed three times in 1 xPBS and postfixed in 1% osmic acid for 1 h at 4degC. Then, gradient dehydration was performed sequentially with 30%, 50%, 75%, 95%, and 100% ethanol for 10 min. Subsequently, the slides were dried to temperature with a CO2 critical-point dryer (Eiko HCP-2, Hitachi). Finally, all of the dried specimens were mounted on aluminum stubs, sputter-coated by an ionic sprayer meter (Eiko E-1020, Hitachi), and analyzed by SEM (Hitachi S3400).

For transmission electron microscopy (TEM), 1.0 mL of the sperm samples was washed routinely and centrifuged at 400 x g for 15 min. Then, the seminal plasma was removed, and the sperm pellets were fixed in 3% glutaraldehyde. Next, the samples were postfixed in 1% buffered OsO4, dehydrated through gradient acetone solutions, and embedded in Epon 812. It was necessary to make the samples into half-thin slices (800 nm) to localize the sperm under the light microscope. Finally, the ultrathin sections (80 nm) were double-stained with lead citrate and uranyl acetate before being observed and photographed via TEM (TECNAI G2 F20, Philips).

2.6 Isolation of human and mouse spermatogenic cells

Spermatogenic cells were obtained through cell diameter/density at unit gravity using the STA-PUT velocity sedimentation method. In brief, human and mouse germ cells were extracted from the testicular biopsy tissues of male adults and adult C57BL/6 male mice. Next, spermatogenic cells were resuspended in 25 ml of 0.5% BSA solution and filtered through an 80 mm mesh to remove cell aggregates. After passage through a mesh filter, the cells were resuspended in buffer containing 0.5% BSA and loaded in an STA-PUT velocity sedimentation cell separator (ProScience) for gradient separation. Several germ cell populations were collected for subsequent analysis.

2.7 Co-immunoprecipitation

Initially, the extracted proteins from human testes were incubated with 7 μ l of target antibodies overnight at 4 °C. Subsequently, the mixture of each sample was added to a microcentrifuge tube containing 40 μ l of prewashed Protein A/G magnetic beads (88803, Invitrogen) and incubated for 2 h at room temperature with constant rotation. After washing with 1 \times PBS three times, the coimmunoprecipitated proteins were eluted with standard 5 \times SDS sample buffer and heated for 10 min at 100°C. Finally, the co-immunoprecipitants were separated on 10% SDS-polyacrylamide gels and PVDF membranes for immunoblot analysis, as described above.

3 RESULTS

3.1 Identification of a recurrent *CFAP47* missense variant in two unrelated infertile men

Two asthenoteratozoospermia patients were recruited for our study. A recurrent missense mutation of c.1414G>A [p.V472M] in *CFAP47* were identified in these patients by WES (Figure 1a). Then, Sanger sequencing confirmed this missense mutation in patients and unaffected parents, implying that *CFAP47* mutation was inherited from their mothers (Figure 1a). Moreover, this *CFAP47* mutation has an extremely low allele frequency in public databases (Table 1) and was predicted to be damaged through the prediction of SIFT, PolyPhen-2, and M-CAP (Table 1). Subsequent sequence alignment analysis found that this amino acid was conserved in multiple species (Figure 1b). These findings indicate that this hemizygous mutation in *CFAP47* might be the potential pathogenic factor for the infertility phenotype of patients.

3.2 Presentation of defective sperm flagellum and head in two infertile patients

To confirm the two patients' detailed phenotypes, we performed semen analysis according to WHO guidelines. The results indicated dramatic decreases in sperm motility and morphological abnormalities in both patients (Table 1). Papanicolaou staining and SEM were further used to analyze sperm morphology. Compared to normal controls, the spermatozoa from patients exhibited a typical MMAF phenotype, including absent, short, and coiled flagella (Figure 2a, b). Noticeably, a defect was observed in the conjunction between the midpiece and principal piece (Figure 2b). To further confirm whether this disruption is involved in the sperm annulus, we detected the expression and localization of SEPTIN4, as a marker of the sperm annulus, by immunofluorescence staining in the patients' sperm (Kissel et al., 2005). As expected, the SEPTIN4 signal was located in the annulus in normal control but was almost absent in patients (Figure 3a), suggesting that *CFAP47* might also be related to the sperm annulus formation.

TEM was performed to investigate the ultrastructure of spermatozoa. In contrast with the well-organized peri-axonemal and axonemal structures in the sperm flagella from normal control, the sperm flagella of patients showed severe disorganization of the peri-axonemal and '9 + 2' axonemal arrangement, the absence of central or peripheral microtubules in the sperm flagella and the disorganized arrangement of mitochondrial sheaths and dense fibers around the axoneme (Figure 2c). Strikingly, typically swollen mitochondria were present in the middle piece (Figure 2c). Based on this phenomenon, COXIV, as a marker of mitochondrial sheath integrity, was used to analyze defects in the mitochondrial sheath (Böttinger et al., 2013). In control sperm, COXIV localized to the midpiece of sperm flagella, but it disappeared completely in the sperm of patients (Figure 3c). Intriguingly, most patients' spermatozoa exhibited abnormally shaped heads, and the nuclei in most sperm of the patients were irregular as well as more unconsolidated than those of the control. Additionally, the majority of the acrosomes were small or even absent in the sperm heads of the patients (Figure 2c). Immunofluorescence staining of PNA also demonstrated acrosomeless spermatozoa or disrupted acrosomes in the sperm of patients (Figure 3b). All evidence indicates that *CFAP47* mutation contributes not only to the MMAF phenotype but also to abnormalities in the sperm head and annulus.

3.3 The negative effect of this missense variant on *CFAP47* expression and function

To investigate the impact of this variant on protein structure, PyMOL Viewer software was used to visualize the effects of altered residues on protein-structure models (Figure 4a). A predicted structure of *CFAP47* with the residues 1-754. Mutant V472M showed it may affect the stability of the original β -sheet region for

methionine occupied more space than valine. This may indicate the structure of CFAP47 was disordered. To further determine the impact of c.1414G>A on *CFAP47* expression, we detected CFAP47 expression in the spermatozoa of the two patients. CFAP47 expression was distributed in flagella in control spermatozoa, while CFAP47 staining was barely detected in the spermatozoa of patients (Figure 4c). Meanwhile, the western blotting showed similar results of significantly decreased protein expression of CFAP47 in the patients' sperm lysates compared to the fertile control (Figure 4b).

As *CFAP47* is regarded as an MMAF-associated gene (Liu et al., 2021), STRING analysis was used to predict which known MMAF genes CFAP47 may interact with. The result revealed that CFAP47 may be connected with CFAP69 (<https://cn.string-db.org/>) (Figure 5a). To confirm this assumption, co-immunoprecipitation was performed, and the result verified binding between CFAP47 and CFAP69 in human testis lysates (Figure 5b). In addition, a previous study demonstrated that CFAP47 regulated and interacted with CFAP65 (Liu et al., 2021). The expression levels of these two proteins were validated to be sharply reduced in the sperm of the two patients compared to the normal control via immunofluorescence staining and western blotting (Figure 5c). In addition, the immunofluorescence assay confirmed the colocalization of CFAP47 with CFAP65 and CFAP69 in mouse (Figure S1) spermatogenic cells at different stages, as well as mouse testis sections (Figure S2). Collectively, the interactions between CFAP47 and its interactors may play a pivotal role in sperm morphology.

3.4 Outcomes of intracytoplasmic sperm injection (ICSI) in patients carrying *CFAP47* mutation

ICSI is a commonly used assisted reproductive technology (ART) to help sterile patients (15). ICSI cycles were attempted for our patients, and written informed consent was obtained for the procedure (Table 2). For patient A, his wife was followed up for one ICSI cycle—with eight oocytes retrieved after GnRH treatment. Five MII was collected, and one 8 II was transferred. Regrettably, his wife has not succeeded in pregnancy. For patient B, his wife underwent a long gonadotrophin-releasing hormone (GnRH) agonist protocol in the first cycle. Six oocytes were retrieved, 4 mature oocytes (metaphase II, MII) were successfully microinjected, and finally, 1 oocyte were normally fertilized (1PN/injected oocytes = 25%). Following extended culture, we obtained one available D3 embryo that failed to develop after being transferred. After this progress, this couple continues the second cycle and chooses the antagonist protocol. We retrieved three metaphase II oocytes and injected them; however, they failed to develop after reaching the available D3 stage. However, a previous study reported satisfactory ICSI outcomes of a loss-of-function mutation in *CFAP47* in humans and male mice (12). We speculated that additional female risk factors for infertility should not be excluded, and more cases need to be investigated to clarify the role of this mutation in ICSI outcomes.

4 DISCUSSION

Sex chromosomes play a key factor in sex determination and reproductive function (Skaletsky et al., 2003). Other than genes located in the autosomal chromosome, sex chromosome genes lack corresponding alleles. Therefore, harmful mutations in sex chromosome genes have a direct impact on male infertility occurrence. To date, limited genetic causes in sex chromosomes have been acknowledged. For example, azoospermia factor (AZF), located on the long arm of the Y chromosome, is composed of AZFa, AZFb, and AZFc (Muller et al., 2008). Previous studies have revealed that AZF microdeletion is related to NOA and severe oligospermia (Yoshida et al., 2014; Navarro-Costa et al., 2010; Colaco et al., 2018). *Deleted in azoospermia 1 (DAZ1)*, *ubiquitin-specific peptidase 9 Y-linked (USP9Y)*, and *RNA binding motif protein Y-linked family 1 member A1 (RBM1)* in the AZF region are identified as candidate causative genes in spermatogenesis. Similar to the Y chromosome, the X chromosome contains genes with exclusive or predominant expression in the testis. Partial deletion of *testis expressed 11 (TEX11)* leads to azoospermia due to meiotic arrest; mutations in *androgen receptor (AR)* attenuate AR regulation of target gene expression and cause oligozoospermia and azoospermia; dysfunction of adhesion G protein-coupled receptor G2 (ADGRG2) results in a buildup of fluid within the testis and an accumulation of spermatozoa within the efferent ducts; *Dynein axonemal assembly factor 6 (DAAF6)* is involved in the assembly of the dynein arm of the ciliary axoneme, and defects in this gene lead to primary ciliary dyskinesia (PCD). Hence, more sex chromosome gene pathogenicity and

biological functions in male reproduction need to be explored.

A previous study on an animal model reported a necessary role of *Cfap47* in spermatogenesis in mice, and their patients were infertile, characterized by abnormal sperm motility and morphology. However, the phenotype and genotype of *CFAP47* in humans have not been comprehensively studied, and the underlying mechanism by which *CFAP47* regulates reproductive biology is limited. In the present study, we detected a novel recurrent missense mutation of *CFAP47*, which is located in the X chromosome, in two sterile patients from two unrelated families. Further in vitro experiments confirmed the pathogenicity of this mutation. By a comprehensive morphology analysis, we first suggested that *CFAP47* mutation is linked to abnormal annulus and aberrations in sperm morphology either in the head or flagellum. More importantly, we explored the interacting proteins of CFAP47 and investigate the molecular mechanism of CFAP47 in sperm morphology. Interestingly, CFAP69 and CFAP65, known MMAF pathogenic genes, are required for flagella assembly and stability in sperm cells. Wang et al. reported that CFAP65 is expressed in the acrosome area and flagellar midpiece in normal human spermatozoa, and CFAP69 is localized to the sperm flagellum. We thus speculated that CFAP47 may be involved in spermatogenesis by interacting with CFAP65 and CFAP69. Moreover, damaged expression of CFAP65 and CFAP69 was detected in the sperm of the patients. Additionally, the co-expression of CFAP47 with CFAP65 and CFAP69 in various spermatogenic spermatids in the testes of humans and mice during spermatogenesis has been presented. These findings indicate a potential role of CFAP47 in regulating spermatogenesis through interacting with CFAP65 and CFAP69. Our study expands the mutational and phenotypic spectrum of *CFAP47* and strongly elucidates the important role of *CFAP47* in male reproduction.

In summary, our study identified a novel missense mutation in *CFAP47* in two infertile male patients with various sperm morphology abnormalities. Our work presented more detailed information on the pathogenesis of *CFAP47* -mutated MMAF and provided direct evidence that suggests the involvement of *CFAP47* in spermatogenesis.

ACKNOWLEDGMENTS

The authors thank the patients and their families for their interest and cooperation. The authors would like to thank the Analytical and Testing Center of Sichuan University for the morphology characterization, and the authors would be grateful to Guiping Yuan for her help with TEM images and Yi He for his help with SEM images. This work was supported by the Science and Technology Department of Sichuan Province (2021YFS0207) and the Health Commission of Sichuan Province (20PJ073).

CONFLICTS OF INTEREST

The authors declare no conflicts of interest.

REFERENCES

- Auguste, Y., Delague, V., Desvignes, J. P., Longepied, G., Gnisci, A., Besnier, P., Levy, N., Beroud, C., Megarbane, A., Metzler-Guillemain, C., & Mitchell, M. J. (2018). Loss of Calmodulin- and Radial-Spoke-Associated Complex Protein CFAP251 Leads to Immotile Spermatozoa Lacking Mitochondria and Infertility in Men. *American Journal of Human Genetics*, 103(3), 413–420. <https://doi.org/10.1016/j.ajhg.2018.07.013>
- Ben Khelifa, M., Coutton, C., Zouari, R., Karaouzène, T., Rendu, J., Bidart, M., Yassine, S., Pierre, V., Delaroche, J., Hennebicq, S., Grunwald, D., Escalier, D., Pernet-Gallay, K., Jouk, P. S., Thierry-Mieg, N., Touré, A., Arnoult, C., & Ray, P. F. (2014). Mutations in DNAH1, which encodes an inner arm heavy chain dynein, lead to male infertility from multiple morphological abnormalities of the sperm flagella. *American Journal of Human Genetics*, 94(1), 95–104. <https://doi.org/10.1016/j.ajhg.2013.11.017>
- Beurois, J., Martinez, G., Cazin, C., Kherraf, Z. E., Amiri-Yekta, A., Thierry-Mieg, N., Bidart, M., Petre, G., Satre, V., Brouillet, S., Touré, A., Arnoult, C., Ray, P. F., & Coutton, C. (2019). CFAP70 mutations lead to male infertility due to severe astheno-teratozoospermia. A case report. *Human Reproduction*, 34(10), 2071–2079. <https://doi.org/10.1093/humrep/dez166>

- Böttlinger, L., Guiard, B., Oeljeklaus, S., Kulawiak, B., Zufall, N., Wiedemann, N., Warscheid, B., van der Laan, M., & Becker, T. (2013). A complex of Cox4 and mitochondrial Hsp70 plays an important role in the assembly of the cytochrome c oxidase. *Molecular Biology of the Cell* , 24(17), 2609–2619.<https://doi.org/10.1091/mbc.E13-02-0106>
- Colaco, S., & Modi, D. (2018). Genetics of the human Y chromosome and its association with male infertility. *Reproductive Biology and Endocrinology* , 16(1), 14.<https://doi.org/10.1186/s12958-018-0330-5>
- Coutton, C., Vargas, A. S., Amiri-Yekta, A., Kherraf, Z. E., Ben Mustapha, S. F., Le Tanno, P., Wambergue-Legrand, C., Karaouzène, T., Martinez, G., Crouzy, S., Daneshpour, A., Hosseini, S. H., Mitchell, V., Halouani, L., Marrakchi, O., Makni, M., Latrous, H., Kharouf, M., Deleuze, J. F., Boland, A., ... Ray, P. F. (2018). Mutations in CFAP43 and CFAP44 cause male infertility and flagellum defects in *Trypanosoma* and human. *Nature Communications* , 9(1), 686.<https://doi.org/10.1038/s41467-017-02792-7>
- Davis-Dao, C. A., Tuazon, E. D., Sokol, R. Z., & Cortessis, V. K. (2007). Male infertility and variation in CAG repeat length in the androgen receptor gene: a meta-analysis. *The Journal of Clinical Endocrinology and Metabolism* , 92(11), 4319–4326.<https://doi.org/10.1210/jc.2007-1110>
- Ferlin, A., Bettella, A., Tessari, A., Salata, E., Dallapiccola, B., & Foresta, C. (2004). Analysis of the DAZ gene family in cryptorchidism and idiopathic male infertility. *Fertility and Sterility* , 81(4), 1013–1018.<https://doi.org/10.1016/j.fertnstert.2003.08.053>
- Gameiro, S., & Finnigan, A. (2017). Long-term adjustment to unmet parenthood goals following ART: a systematic review and meta-analysis. *Human Reproduction Update* , 23(3), 322–337. <https://doi.org/10.1093/humupd/dmx001>
- He, X., Li, W., Wu, H., Lv, M., Liu, W., Liu, C., Zhu, F., Li, C., Fang, Y., Yang, C., Cheng, H., Zhang, J., Tan, J., Chen, T., Tang, D., Song, B., Wang, X., Zha, X., Wang, H., Wei, Z., ... Cao, Y. (2019). Novel homozygous CFAP69 mutations in humans and mice cause severe asthenoteratospermia with multiple morphological abnormalities of the sperm flagella. *Journal of Medical Genetics* , 56(2), 96–103.<https://doi.org/10.1136/jmedgenet-2018-105486>
- He, X., Liu, C., Yang, X., Lv, M., Ni, X., Li, Q., Cheng, H., Liu, W., Tian, S., Wu, H., Gao, Y., Yang, C., Tan, Q., Cong, J., Tang, D., Zhang, J., Song, B., Zhong, Y., Li, H., Zhi, W., ... Cao, Y. (2020). Biallelic Loss-of-function Variants in CFAP58 Cause Flagellar Axoneme and Mitochondrial Sheath Defects and Asthenoteratozoospermia in Humans and Mice. *American Journal of Human Genetics* , 107(3), 514–526.<https://doi.org/10.1016/j.ajhg.2020.07.010>
- Inaba K. (2011). Sperm flagella: comparative and phylogenetic perspectives of protein components. *Molecular Human Reproduction* , 17(8), 524–538.<https://doi.org/10.1093/molehr/gar034>
- Jiao, S.Y., Yang, Y.H. and Chen, S.R. (2021). Molecular genetics of infertility: loss-of-function mutations in humans and corresponding knockout/mutated mice. *Human Reproduction Update* , 27(1), 154–189.<https://doi.org/10.1093/humupd/dmaa034>
- Kissel, H., Georgescu, M. M., Larisch, S., Manova, K., Hunnicutt, G. R., & Steller, H. (2005). The Sept4 septin locus is required for sperm terminal differentiation in mice. *Developmental Cell* , 8(3), 353–364.<https://doi.org/10.1016/j.devcel.2005.01>
- Kleiman, S. E., Almog, R., Yogev, L., Hauser, R., Lehavi, O., Paz, G., Yavetz, H., & Botchan, A. (2012). Screening for partial AZFa microdeletions in the Y chromosome of infertile men: is it of clinical relevance?. *Fertility and Sterility* , 98(1), 43–47.<https://doi.org/10.1016/j.fertnstert.2012.03.034>
- Li, W., Wu, H., Li, F., Tian, S., Kherraf, Z. E., Zhang, J., Ni, X., Lv, M., Liu, C., Tan, Q., Shen, Y., Amiri-Yekta, A., Cazin, C., Zhang, J., Liu, W., Zheng, Y., Cheng, H., Wu, Y., Wang, J., Gao, Y., ... Zhang, F. (2020). Biallelic mutations in *CFAP65* cause male infertility with multiple morphologi-

- cal abnormalities of the sperm flagella in humans and mice. *Journal of Medical Genetics* , 57 (2), 89–95. <https://doi.org/10.1136/jmedgenet-2019-106344>
- Liu, C., Tu, C., Wang, L., Wu, H., Houston, B. J., Mastroianni, F. K., Zhang, W., Shen, Y., Wang, J., Tian, S., Meng, L., Cong, J., Yang, S., Jiang, Y., Tang, S., Zeng, Y., Lv, M., Lin, G., Li, J., Saiyin, H., ... Zhang, F. (2021). Deleterious variants in X-linked CFAP47 induce asthenoteratozoospermia and primary male infertility. *American Journal of Human Genetics* , 108(2), 309–323. <https://doi.org/10.1016/j.ajhg.2021.01.002>
- Mueller, J. L., Mahadevaiah, S. K., Park, P. J., Warburton, P. E., Page, D. C., & Turner, J. M. (2008). The mouse X chromosome is enriched for multicopy testis genes showing postmeiotic expression. *Nature Genetics* , 40 (6), 794–799. <https://doi.org/10.1038/ng.126>
- Navarro-Costa, P., Gonçalves, J., & Plancha, C. E. (2010). The AZFc region of the Y chromosome: at the crossroads between genetic diversity and male infertility. *Human Reproduction Update* , 16(5), 525–542. <https://doi.org/10.1093/humupd/dmq005>
- Paff, T., Loges, N. T., Aprea, I., Wu, K., Bakey, Z., Haarman, E. G., Daniels, J., Sistermans, E. A., Bogunovic, N., Dougherty, G. W., Höben, I. M., Große-Onnebrink, J., Matter, A., Olbrich, H., Werner, C., Pals, G., Schmidts, M., Omran, H., & Micha, D. (2017). Mutations in PIH1D3 Cause X-Linked Primary Ciliary Dyskinesia with Outer and Inner Dynein Arm Defects. *American Journal of Human Genetics* , 100(1), 160–168. <https://doi.org/10.1016/j.ajhg.2016.11.019>
- Patat, O., Pagin, A., Siegfried, A., Mitchell, V., Chassaing, N., Faguer, S., Monteil, L., Gaston, V., Bujan, L., Courtade-Saïdi, M., Marcelli, F., Lalau, G., Rigot, J. M., Mieusset, R., & Bieth, E. (2016). Truncating Mutations in the Adhesion G Protein-Coupled Receptor G2 Gene ADGRG2 Cause an X-Linked Congenital Bilateral Absence of Vas Deferens. *American Journal of Human Genetics* , 99(2), 437–442. <https://doi.org/10.1016/j.ajhg.2016.06.012>
- Skaletsky, H., Kuroda-Kawaguchi, T., Minx, P. J., Cordum, H. S., Hillier, L., Brown, L. G., Repping, S., Pyntikova, T., Ali, J., Bieri, T., Chinwalla, A., Delehaunty, A., Delehaunty, K., Du, H., Fewell, G., Fulton, L., Fulton, R., Graves, T., Hou, S. F., Latrielle, P., ... Page, D. C. (2003). The male-specific region of the human Y chromosome is a mosaic of discrete sequence classes. *Nature* , 423(6942), 825–837. <https://doi.org/10.1038/nature01722>
- Tang, S., Wang, X., Li, W., Yang, X., Li, Z., Liu, W., Li, C., Zhu, Z., Wang, L., Wang, J., Zhang, L., Sun, X., Zhi, E., Wang, H., Li, H., Jin, L., Luo, Y., Wang, J., Yang, S., & Zhang, F. (2017). Biallelic Mutations in CFAP43 and CFAP44 Cause Male Infertility with Multiple Morphological Abnormalities of the Sperm Flagella. *American Journal of Human Genetics* , 100(6), 854–864. <https://doi.org/10.1016/j.ajhg.2017.04.012>
- Tourel, A., Martinez, G., Kherraf, Z.E., Cazin, C., Beurois, J., Arnoult, C., Ray, P.F., and Coutton, C. (2020). The genetic architecture of morphological abnormalities of the sperm tail. *Human Genetics* , 140(1), 21–42. <https://doi.org/10.1007/s00439-00020-02113-x>
- Wang, W., Tian, S., Nie, H., Tu, C., Liu, C., Li, Y., Li, D., Yang, X., Meng, L., Hu, T., Zhang, Q., Du, J., Fan, L., Lu, G., Lin, G., Zhang, F., & Tan, Y. Q. (2021). CFAP65 is required in the acrosome biogenesis and mitochondrial sheath assembly during spermiogenesis. *Human Molecular Genetics* , 30(23), 2240–2254. <https://doi.org/10.1093/hmg/ddab185>
- Yan, Y., Yang, X., Liu, Y., Shen, Y., Tu, W., Dong, Q., Yang, D., Ma, Y., & Yang, Y. (2017). Copy number variation of functional RBMY1 is associated with sperm motility: an azoospermia factor-linked candidate for asthenozoospermia. *Human Reproduction* , 32(7), 1521–1531. <https://doi.org/10.1093/humrep/dex100>
- Yatsenko, A. N., Georgiadis, A. P., Röpke, A., Berman, A. J., Jaffe, T., Olszewska, M., Westernströer, B., Sanfilippo, J., Kurpisz, M., Rajkovic, A., Yatsenko, S. A., Kliesch, S., Schlatt, S., & Tüttelmann, F. (2015). X-linked TEX11 mutations, meiotic arrest, and azoospermia in infertile men. *The New England Journal of Medicine* , 372(22), 2097–2107. <https://doi.org/10.1056/NEJMoa1406192>

Yoshida, K., Makino, T., Yamaguchi, K., Shigenobu, S., Hasebe, M., Kawata, M., Kume, M., Mori, S., Peichel, C. L., Toyoda, A., Fujiyama, A., & Kitano, J. (2014). Sex chromosome turnover contributes to genomic divergence between incipient stickleback species. *PLoS Genetics*, 10(3), e1004223. <https://doi.org/10.1371/journal.pgen.1004223>

Figure legends

Figure 1. Identification of a novel hemizygous variant of X-linked *CFAP47* in asthenoteratozoospermia patients.

(a) Pedigree structure of two families affected asthenoteratozoospermia. The probands are indicated by black arrows. Sanger sequencing confirmed a hemizygous *CFAP47* missense variant in the two families. The position of the variant is indicated by red arrows. (b) *CFAP47* protein structure, localization of variants in the genome, and conservation of mutant amino acids in different species. The red arrow indicates the position of the mutation in our study. The black arrow indicates the mutations that have been reported. The residue V472 is conserved across species.

Figure 2. Sperm morphology and ultrastructure analysis for patients harboring hemizygous *CFAP47* variant.

(a) Papanicolaou staining of spermatozoa obtained from normal control and patients. The patients' sperm showed irregular morphology (scale bars, 5 μm). (b) Detailed defects in sperm were observed in the patient by SEM. The abnormal annulus of patients is indicated by yellow arrows (Scale bars, 5 μm). (c) TEM showed the abnormal ultrastructures of the head and flagellum from the patients' spermatozoa compared normal control (Scale bars, 200 nm).

Figure 3. The characterization of spermatozoa in patients.

(a) Expression of SEPTIN4 was not visible in the sperm annulus of patients compared to normal control (Blue, DAPI; green, SEPTIN4; red, α -tubulin; scale bars, 5 μm). (b) The immunostaining of PNA exhibited imperfect acrosomes in sperm cells of patients compared to the control subject (Blue, DAPI; green, α -tubulin; red, PNA; scale bars, 5 μm). (c) COXIV immunostaining disappeared in the sperm of patients compared to the normal control (Blue, DAPI; green, Septin4; red, α -tubulin; scale bars, 5 μm).

Figure 4. Expression analysis of *CFAP47* in the spermatozoa from a male control individual and men harboring hemizygous *CFAP47* variants.

(a) Structural illustration of the missense mutation in *CFAP47*. (b) Immunoblotting assays revealed that *CFAP47* was dramatically reduced in the spermatozoa from patients harboring *CFAP47* mutation. (c) Immunofluorescence staining reflected a marked decline in *CFAP47* expression in the patients' sperm compared with that in the normal control (Blue, DAPI; red, α -tubulin; green, *CFAP47*; scale bars, 5 μm).

Figure 5. The altered expression of key molecules involved in spermatogenesis is mediated by *CFAP47*.

The protein interaction network was predicted by in silico software STRING for the human *CFAP47* protein. (b) Co-immunoprecipitation analysis showing the binding of *CFAP47* with *CFAP69* using human testis lysates. (c) Immunoblotting assays revealed that *CFAP65* and *CFAP69* were dramatically reduced in the spermatozoa from patients harboring *CFAP47* mutations. (d and e) The signals of *CFAP69* (D) and *CFAP65* (E) were clearly reduced in the sterile patients by fluorescence detection (Blue, DAPI; green, *CFAP47*; red, *CFAP65* and *CFAP69*; scale bars: 5 μm).

Table 1. Semen and variant analysis in the two patients harboring hemizygous a recurrent *CFAP47* mutation

Table 2. Clinical features of the patients' spouses with ICSI treatment

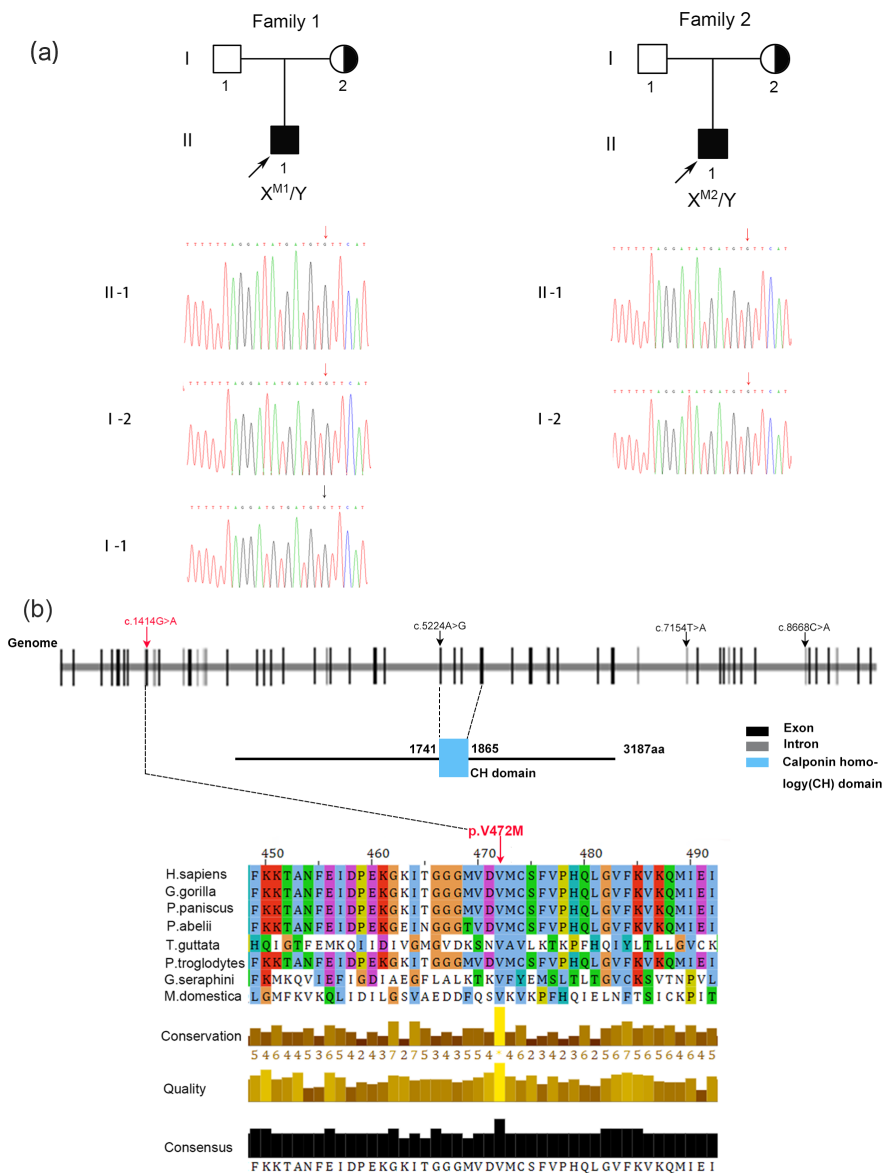
Supplementary information

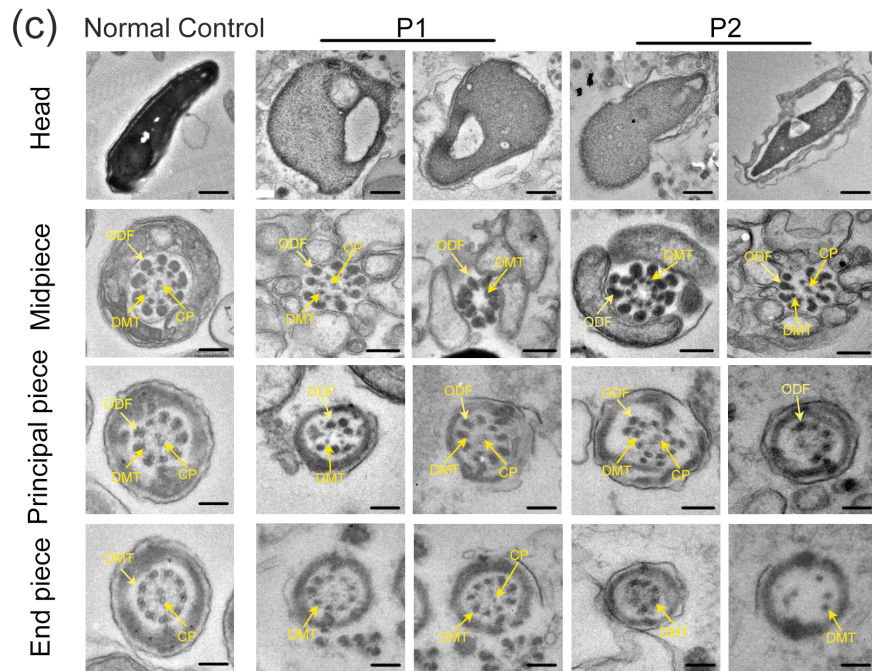
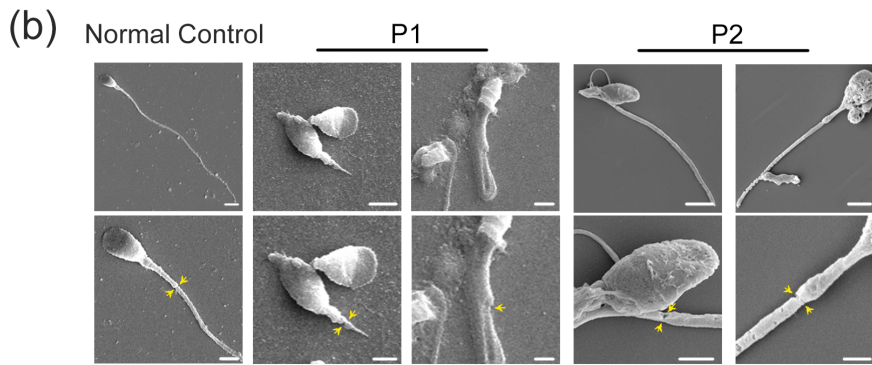
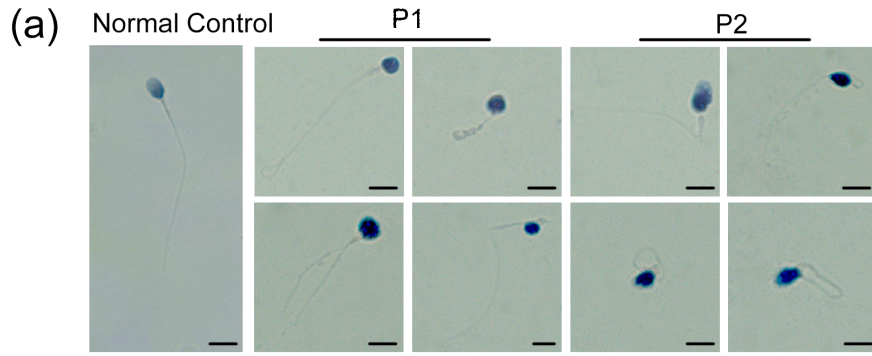
Figure S1. The colocalization of *CFAP47* and *CFAP69/CFAP65* in mouse germ cells.

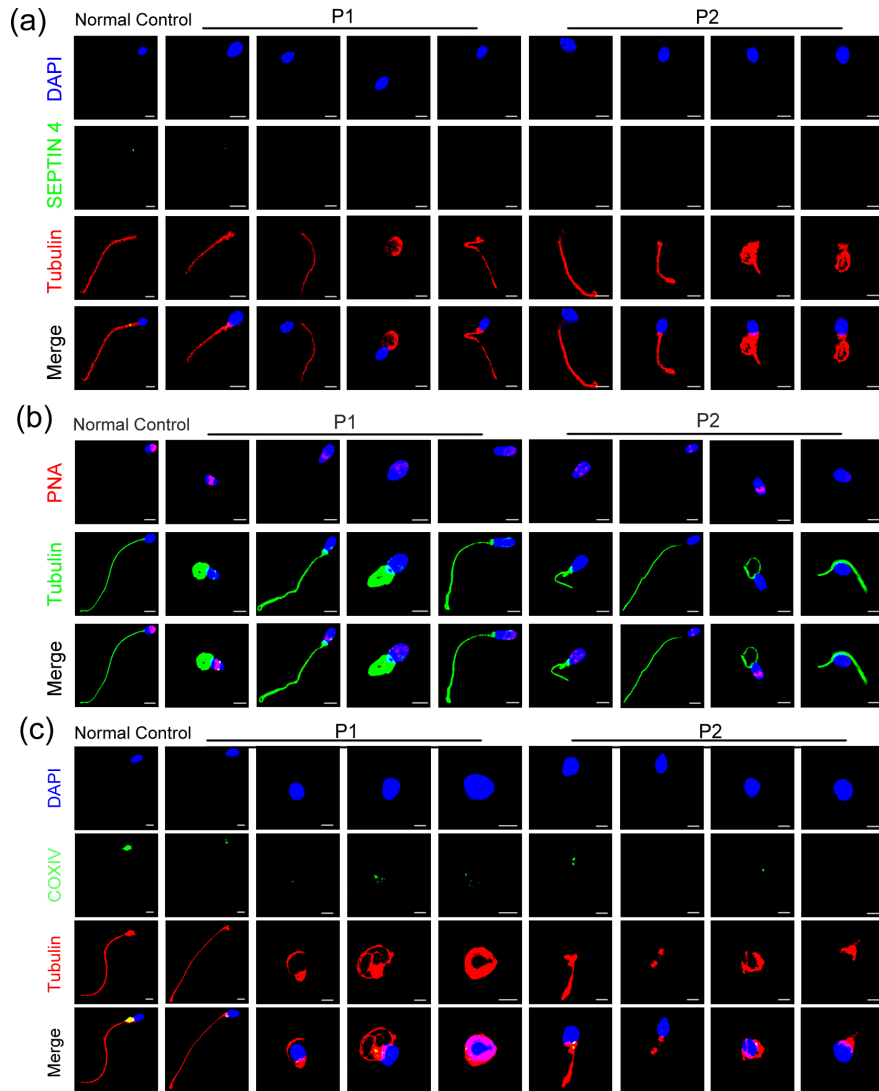
(a and b) Immunofluorescence images showing the colocalization of CFAP47 with CFAP69 (a) and CFAP65 (b) in various germ cells during mouse spermiogenesis (Blue, DAPI; green, CFAP47; red, CFAP65 and CFAP69; scale bars: 5µm).

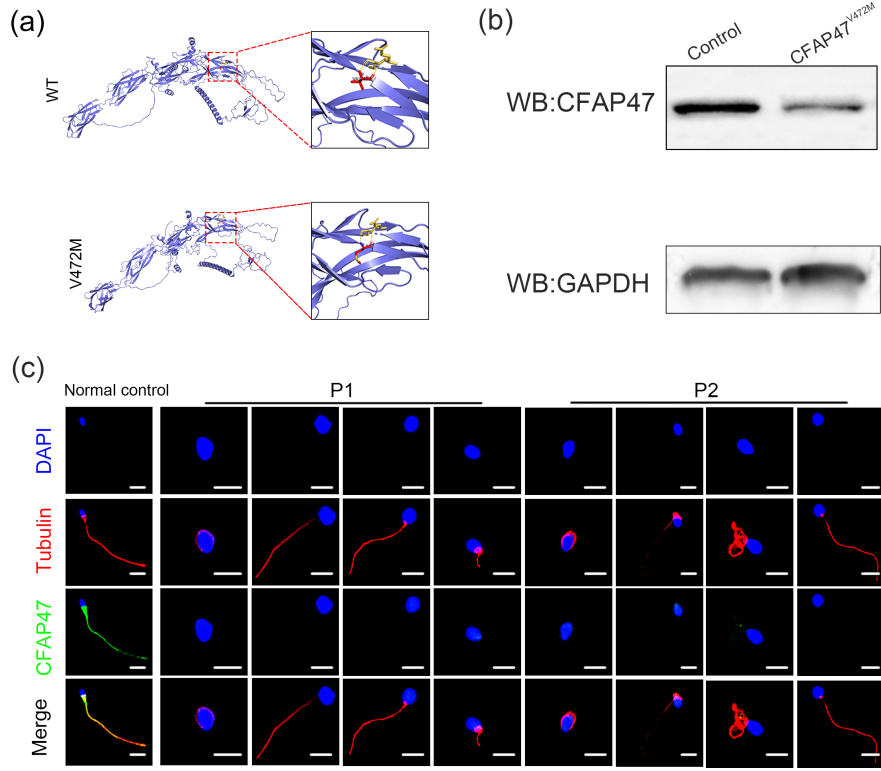
Figure S2. The colocalization of CFAP47 and CFAP69/CFAP65 in mouse testis.

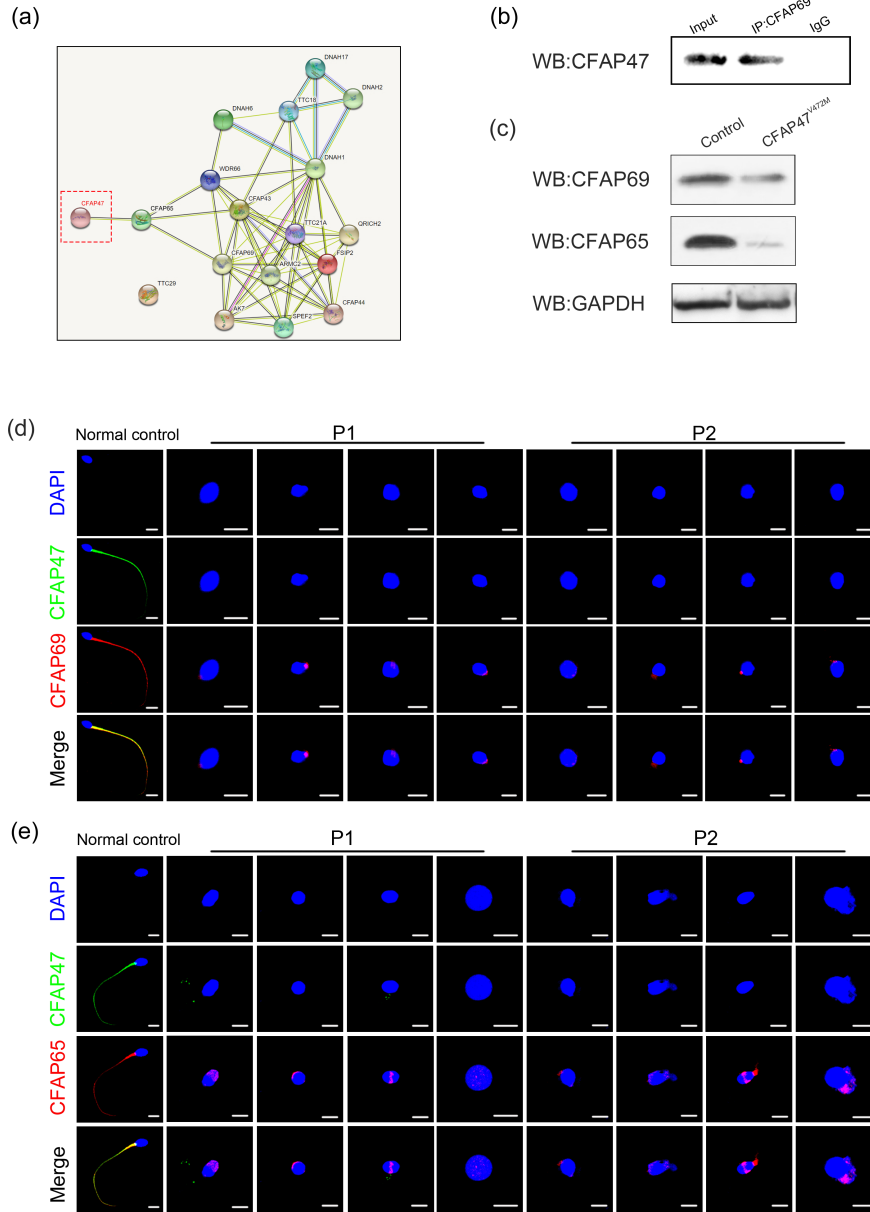
(a and b) Immunofluorescence images showing the colocalization of CFAP47 with CFAP69 (a) and CFAP65 (b) in the testes of mice at different stages (Blue, DAPI; green, CFAP47; red, CFAP65 and CFAP69; scale bars: 5µm).











Hosted file

Table 1.docx available at <https://authorea.com/users/354197/articles/571930-a-novel-recurrent-mutation-in-cfap47-causes-male-infertility-with-asthenoteratozoospermia>

Hosted file

Table 2.docx available at <https://authorea.com/users/354197/articles/571930-a-novel-recurrent-mutation-in-cfap47-causes-male-infertility-with-asthenoteratozoospermia>